ACS OMEGA

Open Access

http://pubs.acs.org/journal/acsodf

Article

Three-Dimensional Surface Stereometric Analysis of Ni−Cu Films with Different Cu Contents

Vali Dalouji* and Samira Goudarzi

Cite This: *ACS Omega* 2024, 9, 4339−4346

Read Online

ACCESS | Metrics & More | Article Recommendations

ABSTRACT: The purpose of this work is a stereometric analysis of Ni−Cu thin films to obtain the three-dimensional (3D) microtexture surface based on atomic force microscopy (AFM). Four Ni−Cu thin films on glass and silicon substrates were prepared by a capacitively coupled RF-PECVD system with a 13.56 MHz power supply. The AFM data of the samples were stereometrically analyzed, and the surface microtexture was determined according to the definition of relevant parameters in the standards ISO 25178−2:2012 and ASME B46.1−2009. All microtexture features can be implemented in numerical programs to simulate advanced microtexture models under specific microstructure and composition conditions. The results can be used to validate theoretical models for predicting or correlating the surface parameters of nanostructures. The Ni−Cu films with 40% Cu have a more irregular surface; hence, the maximum Sq value of the as-deposited Ni−Cu films is about 81.24 μm. The core roughness height Sk is calculated as a difference between two extreme levels (maximal and minimal) of the surface core, for which Ni−Cu films with 40% Cu have a maximum value of 183.4 μm. Since the surface kurtosis (Sku) of all sample films was lower than 7, there are very small peaks or valleys on the film surface and for Ni−Cu films with 5% Cu with a value of 3.568. With increasing Cu content, the height distribution histograms of films show more uniform distributions.

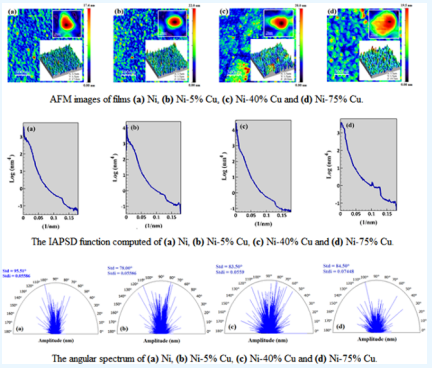
AFM images of films (a) Ni, (b) Ni-5% Cu, (c) Ni-40% Cu and (d) Ni-75% Cu.

The IAPSD function computed of (a) Ni, (b) Ni-5% Cu, (c) Ni-40% Cu and (d) Ni-75% Cu.

The angular spectrum of (a) Ni, (b) Ni-5% Cu, (c) Ni-40% Cu and (d) Ni-75% Cu.

1. INTRODUCTION

The importance of the physical phenomena that occur in thin films is first due to the broad perspective of the application of thin films in practice (ultrafrequency engineering, optoelectronics, microelectronics, etc.) and, second, the possibility of obtaining the information needed to solve some basic problems in solid state and surface physics. The Ni−Cu thin films have been the subject of many studies. Several interesting features of the Ni−Cu system have been reported.[1−5] As is known, optical properties of nanoparticles strongly depend on the morphology of the nanostructure. However, there is a dearth of advanced microtexture and fractal/multifractal analysis. Therefore, it is important to study these structural parameters for practical applications. Recently, advanced studies have contributed to a deeper understanding of the three-dimensional surface microtexture of thin films, which promotes the development of nanomaterials with major technological applications.[6,7] Advanced techniques of characterization are at the center of scientific attention.[8−10] Different studies showed that the three-dimensional surface microtexture can be described using stereometric[11] and fractal/multifractal analyses[12−14] with a minimal set of surface parameters. Imaging by AFM can bring outstanding results in the field of research and analysis of nanostructured surfaces, especially in the case of thin films.[15−17] As the main goal, the 3D surface micromorphology of Ni−Cu thin films was investigated using AFM and stereometric analyses. Details on the experimental techniques and the deposition conditions are given in Section 2. The structural properties were studied by scanning electron microscopy (SEM) (Section 3.1), while the surface roughness was investigated by using atomic force microscopy (AFM) (Section 3.2). The conclusions are presented in Section 4.

2. MATERIALS AND METHODS

2.1. Empirical Techniques. In this article, Ni−Cu nanoparticles with similar amounts of Ni and different amounts of Cu concentration were deposited by a capacitively coupled RF-PECVD system with a 13.56 MHz power supply. The reactor includes two electrodes with different target sizes of Ni and Cu because the fed electrode was the smaller electrode in the first and second stages of film deposition, respectively. The distance between the nickel and copper targets and the substrate was 6 cm. The body of the stainless steel chamber was connected to the ground through a larger

Received: August 20, 2023
Revised: January 2, 2024
Accepted: January 8, 2024
Published: January 19, 2024

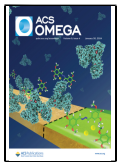

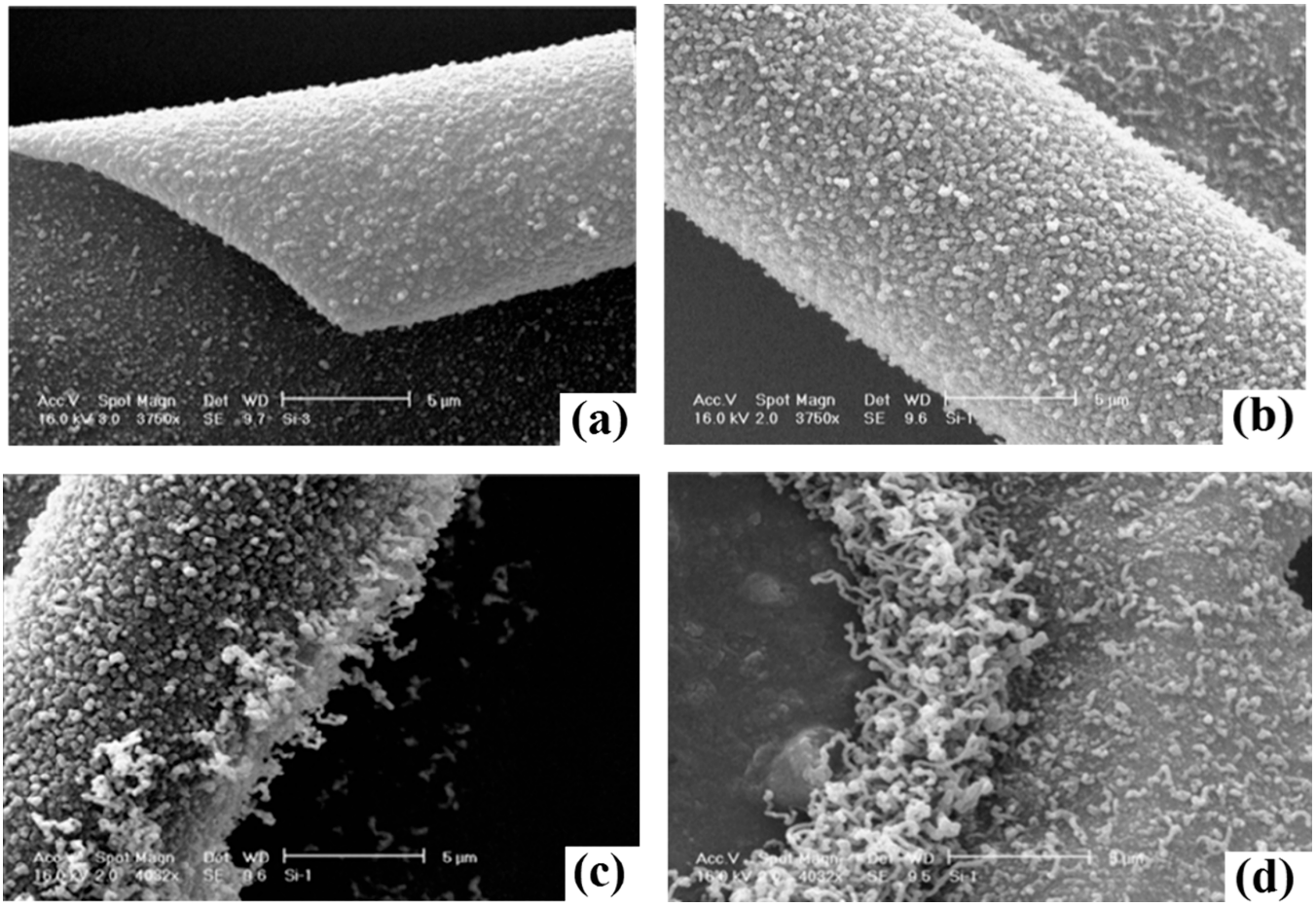

Figure 1. SEM images of the prepared CNTs using (a) Ni, (b) Ni-5% Cu, (c) Ni-40% Cu, and (d) Ni-75% Cu.

electrode. The entire deposition process was performed at room temperature on a larger electrode on a glass substrate. Before deposition, the chamber was vacuumed up to the base pressure of 10^{-5} mbar, and then the pressure was increased to ambient pressure by acetylene gas. In the first step, the codeposition of the RF sputtering and RF-PECVD, for growth of Ni−Cu nanoparticles, RF power, and the acetylene initial pressure were set at 180 W and 0.045 mbar, 210 W and 0.05 mbar, and 190 W and 0.04 mbar to obtain films with different Cu nanoparticles. The deposition time for Cu deposition was 20 min, and after Cu deposition, the electrode was changed to Ni and sputtering was performed for 2 min with an RF power of 260 W and acetylene initial pressure of 0.03 mbar. The thickness of the films was measured using a Tencor Alpha-step 500 profiler, and the thickness of these films was about 100 nm. In the presented work, structural properties have been described by using SEM. AFM imaging has been used to describe the three-dimensional surface of the sample, and fractal analysis has been performed on the obtained data. The stereometric analysis was made with the SPIP-TM version 6.7.4 software,[18] based on ISO25178−2:2012[19] and ASME B46.1−2009.[20]

2.2. SEM, AFM, and Stereometric Analysis of the 3D Surface Microtexture. Scanning electron microscopy (SEM) is one of the most versatile tools available to investigate and analyze the microstructure morphology and chemical composition characteristics.

The surface of the thin film samples was scanned by scanning electron microscopy (VEGA-TESCAN LMU), and gray scale images were obtained. To study the topography of tissues, an atomic force microscope was used in noncontact mode (Autoprobe CP Research, Veeco; Spring constant: 20−80 N/m) with a scanning speed of 10−20 μm/s and a tip radius of 10 nm; the obtained results were 256 × 256 pixel images. The experimental processes were carried out at room temperature (297 ± 1 K) by the console, where the force−distance curve measurement properties are as follows: Poisson ratio ν = 0.28.22, quality factor Q = 100, width 25 μm, length 180 μm, Young's modulus E = 1.3101 Pa, tip radius 10 nm, thickness 4 μm, and mass density ρ = 2,33 kg/m^3. AFM image processing was performed to obtain three-dimensional surface geometry and microtexture parameters using SPIP-TM version 6.7.4 software based on the ISO 25178−2:2012 and ASME B46.1−2009 standards.

2.3. Statistical Analysis. Statistical analyses were carried out with the GraphPad In-Stat computer software package, version 3.20 (GraphPad, San Diego, CA, USA). In addition, the normal distribution of quantitative variables was evaluated with the Kolmogorov−Smirnov test. After the statistical significance was discovered, differences between the two groups were compared using the Mann−Whitney U test. The differences were statistically significant by p = 0.05 or less.

3. RESULTS AND DISCUSSION

3.1. SEM Images Analysis. It is well-known that the morphology of the catalyst films plays an important role in the growth of carbon nanotubes (CNTs) and carbon nanofibers

https://doi.org/10.1021/acsomega.3c06181
ACS Omega 2024, 9, 4339−4346

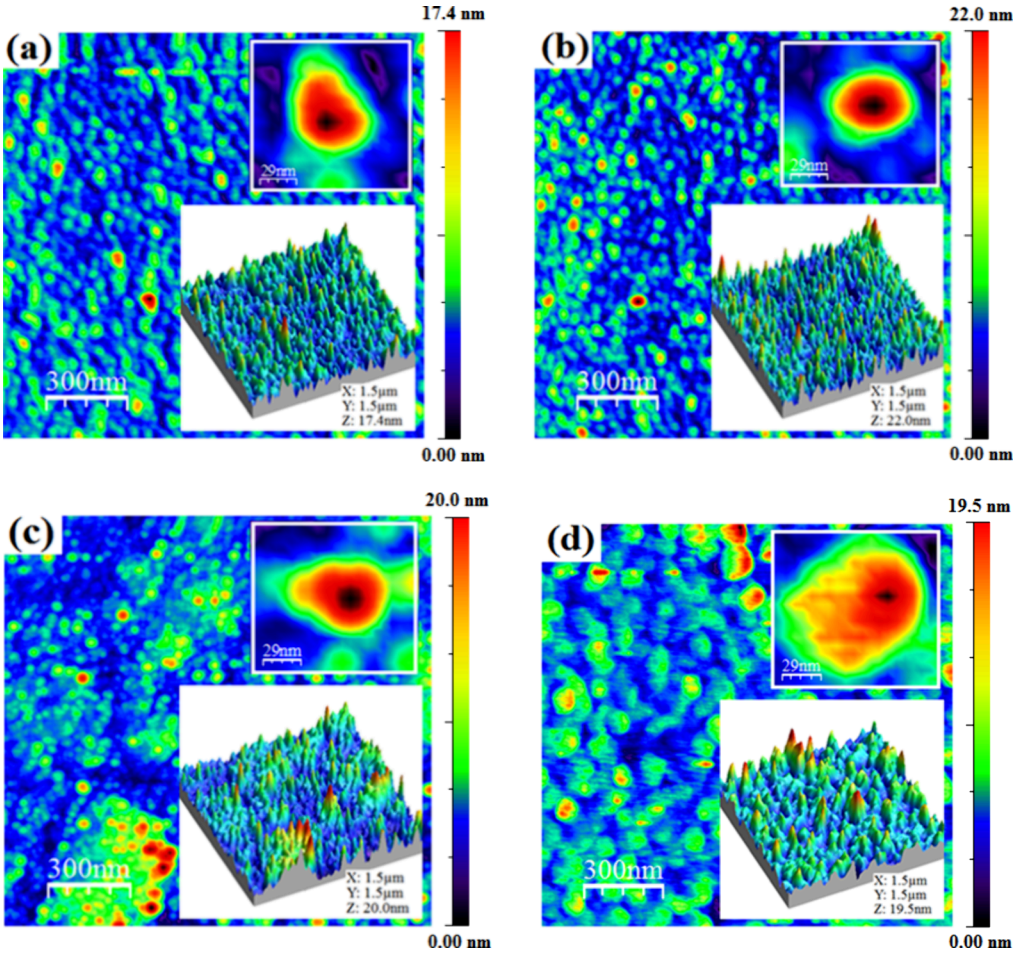

Figure 2. AFM images of films (a) Ni, (b) Ni-5% Cu, (c) Ni-40% Cu, and (d) Ni-75% Cu.

(CNFs).[21] Figure 1a–d shows CNTs for Ni nanoparticles without Cu nanoparticles and with Cu nanoparticles containing 5, 40, and 75% Cu. A scanning electron microscope is a microscope that uses a focused beam of electrons to scan the surface of a sample to create a high-resolution image. Scanning electron microscopy produces images that can reveal information about the surface composition and topography of a material. Scanning electron microscopy images showed that the carbon nanotubes have different diameters, and generally, the average diameter of the grown carbon nanotubes increased with the increase in the percentage of Cu in the thin films. Up to 40% Cu, the CNT uniformity height of nanoparticles is low, and then at more than 40% Cu, the CNT uniformity was increased. One notable feature is the effect of the percentage of Cu on the diameter of CNTs. Eventually, by selection of the Ni nanoparticles as the substrate of Cu nanoparticles, the density and diameter of CNTs can be optimized. As a result, Cu nanoparticles have an important role in the growth of CNTs based on Ni nanoparticles catalysts. This phenomenon can be explained by the decomposition of the hydrocarbon gas on the exposed surfaces of the catalyst particles to release hydrogen and carbon, so that the carbon atoms themselves are dissolved in the particles. Dissolved carbon diffuses through the particle and is deposited at the distal end to form the body of the carbon fiber. Also, if we assume a direct relationship between the average nanoparticle sizes and the diameter of the grown carbon nanotubes, it can be suggested that the nanoparticles are agglomerated and lead to the formation of more particles during the CNT growth process. Such agglomeration seems to have increased dramatically for films deposited with 75% Cu; consequently, the average diameter of grown CNTs with 75% Cu is much larger than that in other samples.

3.2. AFM Images Analysis. Atomic force microscopy images are used to estimate the average size of nanoparticles, and these images can be used to elucidate many physical properties.[22−24] Figure 2a–d illustrates the 2D and 3D views of the surface AFM analysis of samples. AFM results show that the nanoparticles of Ni−Cu thin films have grown perpendicular to the surface of the substrate (the three-dimensional section of the surface images). The RMS roughnesses of the films with 5, 40, and 75% Cu were found to be about 3.6, 2.2, and 2 nm, respectively. The reduction of RMS roughness indicates aggregation of Cu nanoparticles for thin films containing 5, 40, and 75% Cu. Therefore, it was found that the roughness of the film surface decreases with the increase of the percentage of Cu and the surface of the films becomes smooth and also bright spots appear in AFM images. By increasing the percentage of Cu nanoparticles in the thin films, the surface energy of the films increases and the pores are filled, which in turn suggests aggregation of Cu nanoparticles. From 40 to 75% Cu, the size of nanoparticles increases significantly. The other samples appear to contain particles of the same size but with different concentrations. By adding Ni nanoparticles to this thin film, the surface morphology does not change except for the sample with 75% Cu (Figure 2d)

https://doi.org/10.1021/acsomega.3c06181
ACS Omega 2024, 9, 4339−4346

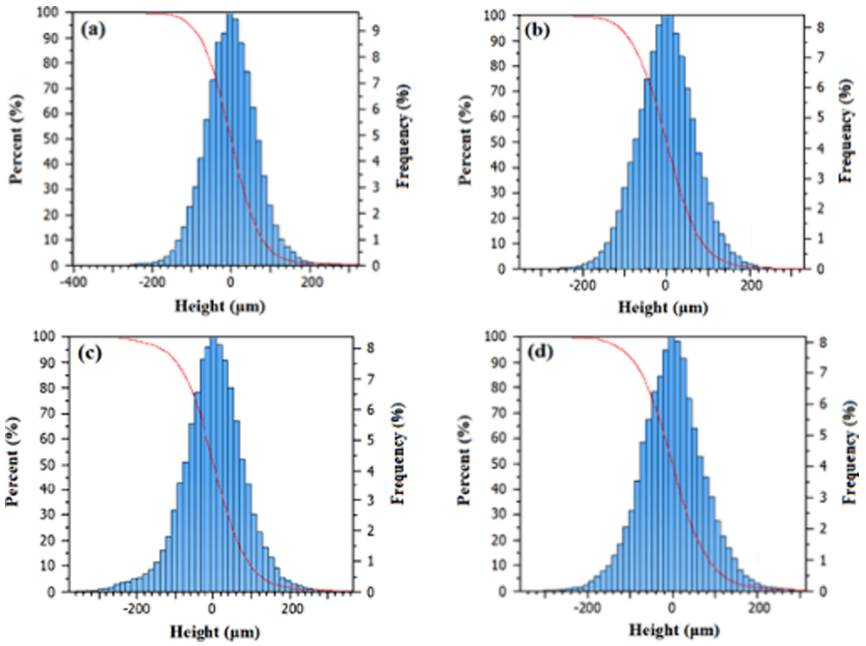

Figure 3. Height distribution histograms (painted in blue color) with their integration curve (painted in red color) for (a) Ni, (b) Ni-5% Cu, (c) Ni-40% Cu, and (d) Ni-75% Cu.

Table 1. Statistical Parameter Values Based on ISO 25178-2:2012 and ASME B46.1-2009 for Analyzed Samples

statistical parameters	symbol	Ni	Ni-5% Cu	Ni-40% Cu	Ni-75% Cu
amplitude parameters					
arithmetic mean height	Sa (μm)	50.02	53.80	61.72	57.45
root mean square height	Sq (μm)	64.55	68.90	81.24	74.40
surface skewness	Ssk	0.03057	−0.0001118	−0.2098	0.06665
surface kurtosis	Sku	4.054	3.568	4.196	3.682
maximum height	Sz (μm)	725.4	680.6	744.3	673.0
maximum valley depth	Sv (μm)	401.5	351.3	377.6	358.8
maximum peak height	Sp (μm)	323.9	329.3	366.7	314.3
hybrid parameters					
area root-mean-square slope	Sdq	0.5525	0.5933	0.4866	0.4728
surface area ratio	Sdr (%)	11.98	13.99	9.101	8.737
reduced summit height	Spk (μm)	72.55	74.68	89.50	84.96
core roughness depth	Sk (μm)	155.6	166.0	183.4	171.2
reduced Valley depth	Svk (μm)	69.31	70.96	107.2	82.55
spatial parameters					
texture direction index	Stdi (mm)	0.05586	0.05586	0.0559	0.07448
dominant radial wavelength	Srw (nm)	0.00063	0.0016	0.00073	0.0012
radial wave index	Srwi	0.00037	0.0006	0.0005	0.00029
functional parameters (volume)					
material volume	Vm(mm^3/mm^2)	0.003624	0.003699	0.004466	0.004183
void volume	Vv(mm^3/mm^2)	0.08245	0.08952	0.1010	0.09743
peak material volume	Vmp(mm^3/mm^2)	0.003624	0.003699	0.004466	0.004183
core material volume	Vmc(mm^3/mm^2)	0.05492	0.0601	0.06619	0.06332
core void volume	Vvc(mm^3/mm^2)	0.07489	0.08152	0.09026	0.08878
pit void volume	Vvv(mm^3/mm^2)	0.00756	0.0080	0.01079	0.008653

where the RMS roughness changes from 2 to 2.2. It was also observed that the RMS roughness changed with the percentage of Cu and the amount of carbon in the layers.

Stereometric analysis was performed based on the AFM data because it provides true three-dimensional information about the surface texture.[25,26] Topography of the surface based on stereometric analysis was described using the SPIP-TM version 6.7.4 software,[18] based on ISO 25178−2:2012[19] and ASME B46.1−2009.[20] The histograms of the height distribution of the AFM images (painted in blue) with their integration curves (painted in red) associated with the images are shown in Figure 3. The height histogram is represented by the number of elements appearing on the surface corresponding to the height of the specified peak along with the material curve of the areal that is placed on the histogram. The height distribution histogram provides information about the flatness

https://doi.org/10.1021/acsomega.3c06181
ACS Omega 2024, 9, 4339−4346

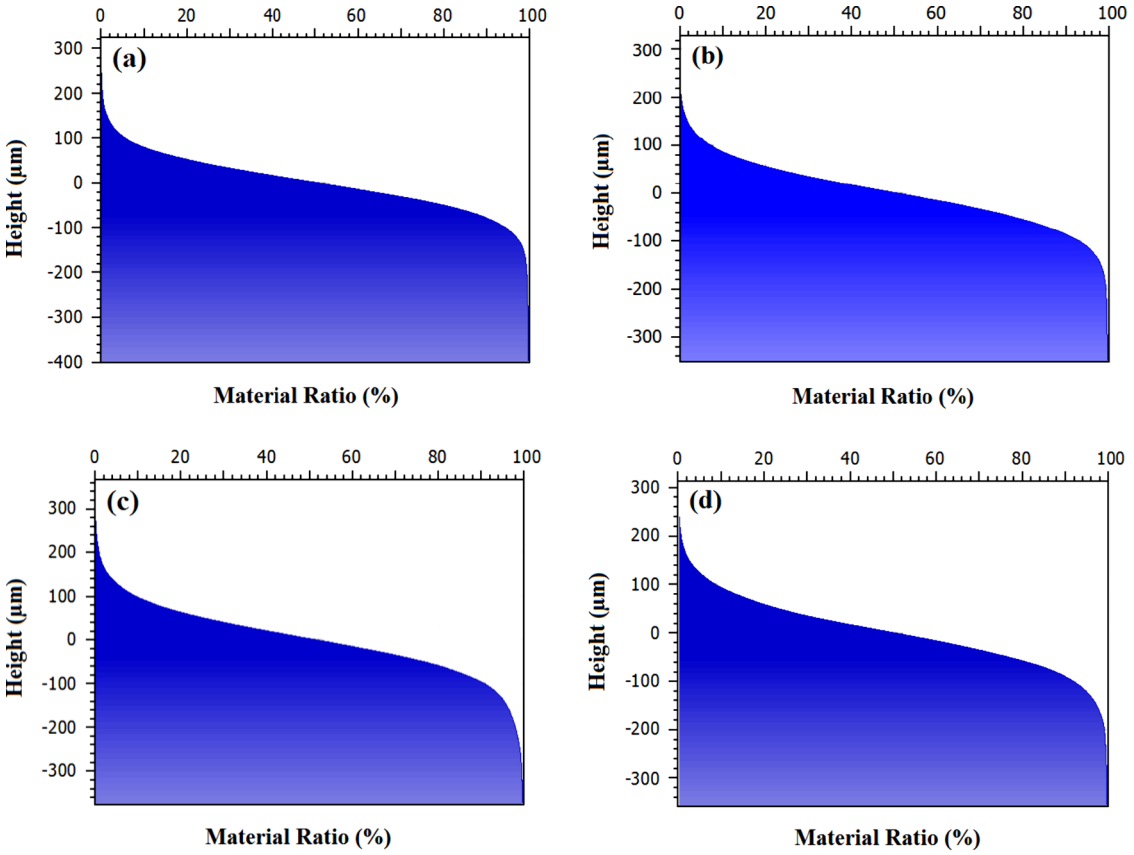

Figure 4. Abbott–Firestone curves for (a) Ni, (b) Ni-5% Cu, (c) Ni-40% Cu, and (d) Ni-75% Cu.

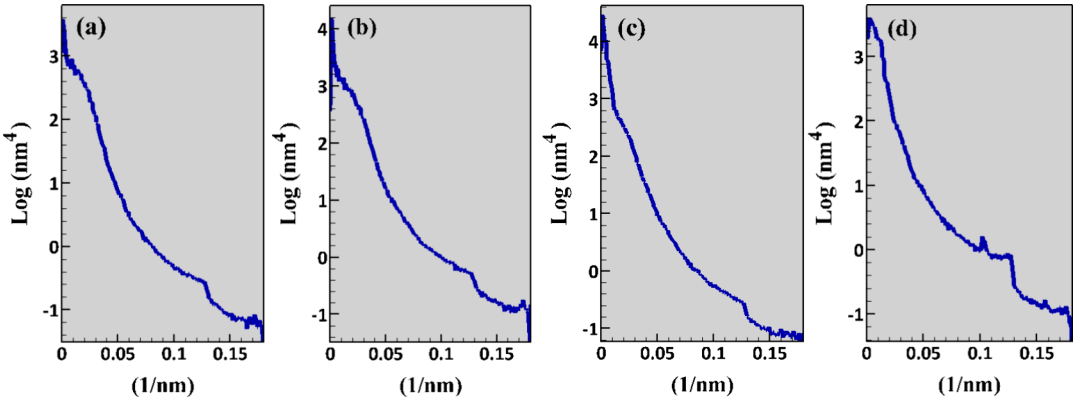

Figure 5. IAPSD function computed of (a) Ni, (b) Ni-5% Cu, (c) Ni-40% Cu, and (d) Ni-75% Cu.

of the film surface. The red diagram shows a curve of an areal material with parameter values of Sk, Svk, and Spk, and these values are presented in Table 1. The histogram peaks are zero for all samples, and the histograms are approximately symmetric around zero. For samples (a) and (b), the height distribution reaches zero at 220 μm, but for samples (c) and (d), the height distribution at 220 μm still existed, and it reaches zero for the height of 280 μm. Therefore, as the Cu percentage increases, the samples become smoother, and the range of height distribution becomes wider.

The Abbott–Firestone curve is shown in Figure 4, which represents the bearing ratio curve. Profile trace integration can calculate the cumulative probability density function of the height of the surface profile, which is mathematically equal to the load ratio curve. Also, these curves show the load-bearing capacity of the surfaces, and a larger area indicates an increase in the load-bearing capacity. As can be seen in Figure 4, most of the material on all of the surfaces lies below the mean surface irregularities. The largest material ratio (%) above the mean surface height is to be observed for films deposited with 75% Cu. It means that such samples show the largest surface area for wetting. In addition, the more irregular surface (Sq = 81.24 μm) was found for films deposited with 40% Cu, and the more regular surface (Sq = 64.55 μm) was found for films deposited with pure Ni.

In Figure 5, the isotropic area power spectral density (IAPSD) functions are given on a logarithmic scale, as extracted from the AFM images shown in Figure 2. The isotropic area power spectral density (IAPSD) function is the APSD (area power spectral density) function integrated for all

https://doi.org/10.1021/acsomega.3c06181
ACS Omega 2024, 9, 4339–4346

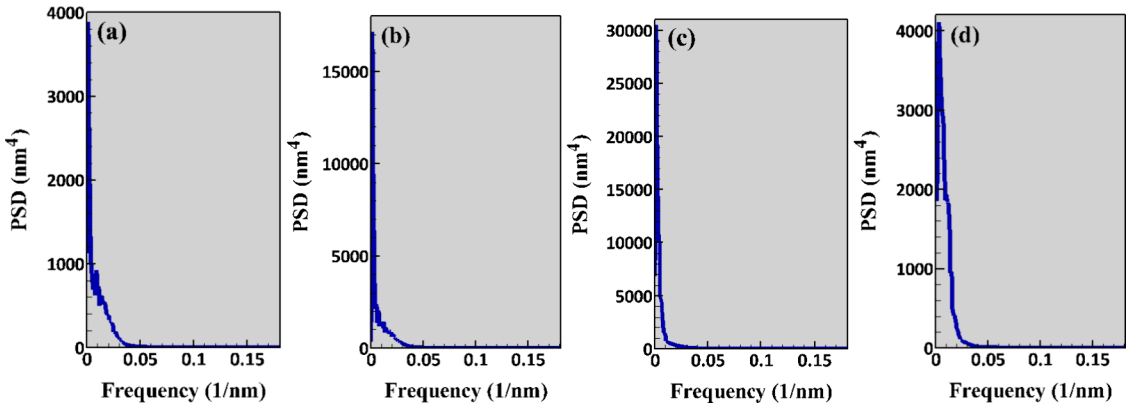

Figure 6. Average X-PSD profile of (a) Ni, (b) Ni-5% Cu, (c) Ni-40% Cu, and (d) Ni-75% Cu.

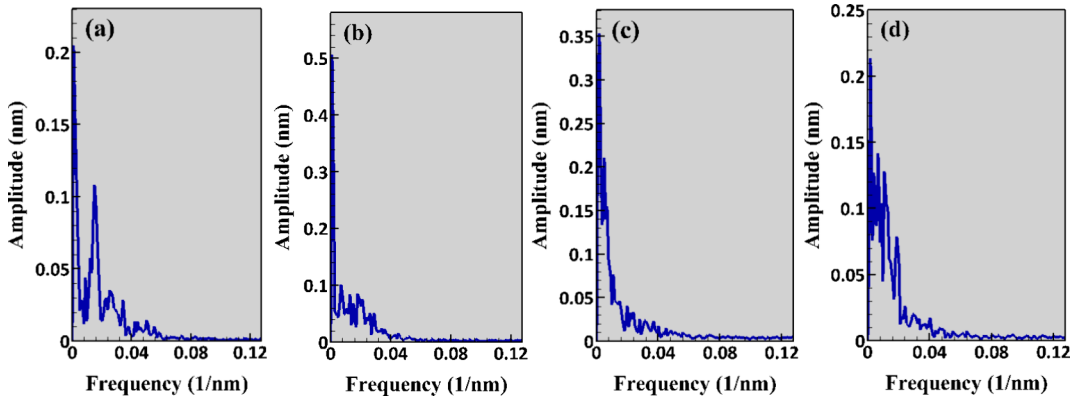

Figure 7. Average X-Fourier profile of (a) Ni, (b) Ni-5% Cu, (c) Ni-40% Cu, and (d) Ni-75% Cu.

angles at the given frequencies (taking into account the inverse wavelength).[18] By increasing the Cu content, up to 40% Cu, IAPSD function values increased systematically, and then over 40% Cu, the values of the IAPSD function were decreased. As seen in Figure 5, all the curves are similar.

The power spectral density (PSD) method is a powerful Fourier technique for surface roughness analysis. This approach enables a better demonstration of the magnitude and significance of surface defects as a function of the spatial frequency of the roughness. This frequency is the inverse of the roughness wavelength. The mean power spectral density (X-PSD) profile curves calculated according to[18] and corresponding to the AFM images in Figure 2 are indicated in Figure 6. As the surface kurtosis (Sku) of all samples is above 3, there are high peaks or valleys on the surface, which are the largest for films deposited with 40% Cu (4.196) and the lowest value for films deposited with 5% Cu (3.568). The one-dimensional FFT (fast Fourier transform) line-averaged functions describe the Fourier amplitude spectrum for the X line and the corresponding amplitude-averaged spectrum. In Figure 7, the average X-Fourier profile curves, associated with the images in Figure 2, according to ref 27, are shown. Average X-PSD and X-Fourier curves confirm the results obtained by fractal analysis.

Figure 8 shows the plots of the angular spectra corresponding to the AFM images in Figure 2. To analyze whether the topography of the sample shows dominant directional patterns, we generated angular spectra for each sample. Angular spectrum diagrams of samples are radial diagrams with relative amplitudes that show the dominant orientation of the surface texture. For any relative amplitude, which is found as the sum of all amplitudes along a given radial line in the Fourier spectrum of the AFM image, the specific features of the surface texture seen in the AFM images are derived based on ISO 25178−2:2012 and ASME B46.1−2009 (Table 1).

Moreover, the radial spectra of all samples are extracted from images in Figure 2 and are presented in Figure 9. A radial spectrum is a scatter plot that shows the range of brightness as a function of the wavelength in images. These plots were generated by the 2D Fourier transform (SPIP-TM version 6.7.4 Software).

Table 1 shows the statistical parameter values of AFM micrographs based on ISO 25178−2:2012 and ASME B46.1−2009. The graphs in Figure 3 show the surface material curve with Sk, Svk, and Spk parameter values, while the fourth diagram is applied to calculate the volume parameters containing Vmp, Vmc, Vvc, and Vvv using the surface material curve. As seen in Table 1, The maximum arithmetic mean value of the vertical deviation from the mean surface (Sa) corresponds to the films deposited with 40% Cu. The surface skewness (Ssk) of films deposited with 5% and 40% Cu is negative (Ssk < 0). The surface kurtosis (Sku) of all the samples is above 3. The sum of the maximum pit height and maximum peak height value is tagged as Sz with the minimum and maximum values of 673.0 and 744.3 μm related to films deposited with 75% and 40% Cu, respectively. In addition, Sp and Sv define the maximum peak height and maximum valley depth values of each film. As it is seen, the maximum value of Sp was obtained for films deposited with 40% Cu and the

https://doi.org/10.1021/acsomega.3c06181
ACS Omega 2024, 9, 4339−4346

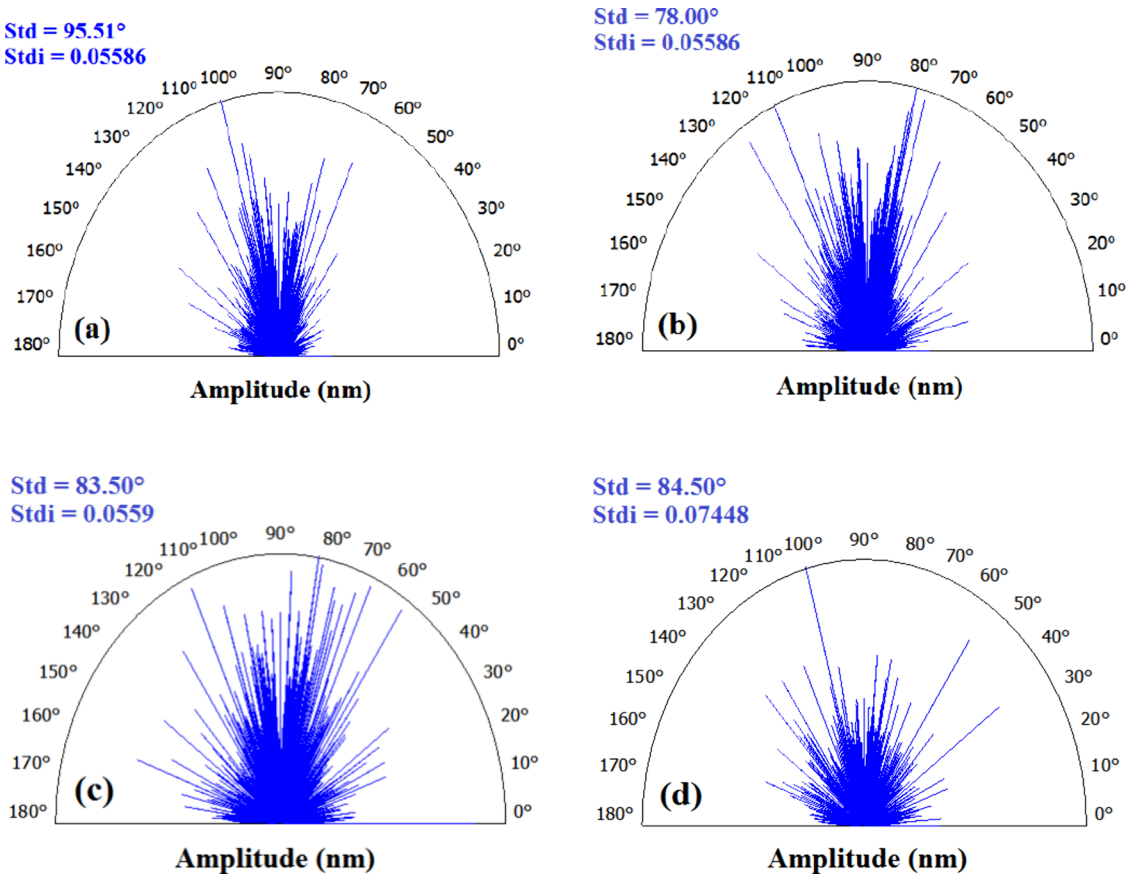

Figure 8. Angular spectrum of (a) Ni, (b) Ni-5% Cu, (c) Ni-40% Cu, and (d) Ni-75% Cu.

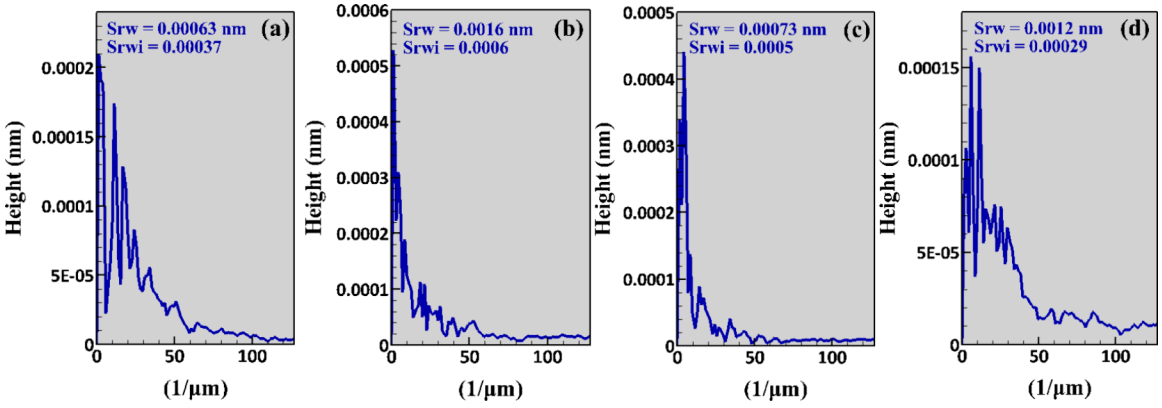

Figure 9. Radial spectrum of (a) Ni, (b) Ni-5% Cu, (c) Ni-40% Cu and (d) Ni-75% Cu.

maximum value of Sv for films deposited with pure Ni. By analysis of the functional parameters in Table 1 and extraction from the ratio curve of the surface materials, it can be seen that the roughness height of the core Sk, which is calculated as the difference between the two extreme levels (maximum and minimum) of the surface core, has the highest value for the films deposited with 40% Cu (183.4 μm) and the lowest for films deposited with pure Ni (155.6 μm). Svk and Spk are abbreviations for the reduction of the Dale height and the reduction of the peak height, the highest value of Svk and Spk corresponding to the films deposited with 40% Cu (107.2 and 89.50 μm, respectively), and their lowest value for films deposited with pure Ni (69.31 and 72.55 μm, respectively).

4. CONCLUSIONS

The 3D surface stereometric analysis of films using the SPIP-TM 6.7.4 software, based on ISO 25178−2:2012 and ASME B46.1−2009, was studied. Also, the variation of the surface morphology was investigated by atomic force microscopy. Based on the data obtained in this study, according to the nanometric changes in the geometry and spatial distribution of the microtextures of the sample surfaces under analysis, it is obvious that topographical geometric features influence the set of relationships between surface and structure in a thin film under different experimental conditions at micrometer and nanometer scales. The measurement and characterization of surface topography can lead to a correct understanding of the

https://doi.org/10.1021/acsomega.3c06181
ACS Omega 2024, 9, 4339−4346

production process concerning physical properties both theoretically and experimentally.

AUTHOR INFORMATION

Corresponding Author

Vali Dalouji − *Department of Physics, Faculty of Science, Malayer University, Malayer, Iran;* orcid.org/0000-0002-1233-5858; Phone: +988132355466; Email: dalouji@yahoo.com

Author

Samira Goudarzi − *Department of Physics, Faculty of Science, Malayer University, Malayer, Iran*

Complete contact information is available at: https://pubs.acs.org/10.1021/acsomega.3c06181

Notes

The authors declare no competing financial interest.

ACKNOWLEDGMENTS

The authors are willing acknowledge Dr. Ali Arman from ACECR- Sharif University Branch for his support in the software data section for this research.

REFERENCES

(1) Kacel, T.; Guittoum, A.; Hemmous, M.; Dirican, E.; Öksüzoglu, R. M.; Azizi, A.; Laggoun, A.; Zergoug, M. Effect of Thickness on the Structural, Microstructural, Electrical and Magnetic Properties of Ni Films Elaborated By Pulsed Electrodeposition on Si Substrate. *Surf. Rev. Lett.* **2018**, *25* (02), 1850058.

(2) Chandesris, D.; Le Fèvre, P.; Magnan, H.; Jaffres, H. Surface EXAFS study of metastable magnetic thin films. *Journal of synchrotron radiation* **2001**, *8* (2), 141−144.

(3) Nacereddine, C.; Layadi, A.; Guittoum, A.; Cherif, S.-M.; Chauveau, T.; Billet, D.; Ben Youssef, J.; Bourzami, A.; Bourahli, M.-H. Structural, electrical and magnetic properties of evaporated Ni/Cu and Ni/glass thin films. *Mater. Sci. Eng.: B* **2007**, *136* (2−3), 197−202.

(4) Bi, Xiaoyang; Xiaowu, Hu; Li, Qinglin Effect of Co addition into Ni film on shear strength of solder/Ni/Cu system: experimental and theoretical investigations. *Mater. Sci. Eng.: A* **2020**, *788*, 139589.

(5) Guevara, Laura; Welsh, Roger; Atwater, Mark A. Parametric effects of mechanical alloying on carbon nanofiber catalyst production in the Ni-Cu system. *Metals* **2018**, *8* (4), 286.

(6) Ţălu, Ştefan. *"Micro and nanoscale characterization of three dimensional surfaces.Basics and applications. Cluj-Napoca."* Napoca Star Publishing House: Romania (2015).

(7) Ţălu, Ştefan, Sebastian, Stach, Shahoo, Valedbagi, Mohammad S., Elahi, Reza, Bavadi. *"Surface morphology of titanium nitride thin films synthesized by DC reactive magnetron sputtering."* (2015).

(8) Kaspar, Pavel; DinaraSobola, Rashid Dallaev; Shikhgasan, Ramazanov; Alois, Nebojsa; Sahar, Rezaee; Lubomír, Grmela Characterization of Fe2O3 thin film on highly oriented pyrolytic graphite by AFM, Ellipsometry and XPS. *Appl. Surf. Sci.* **2019**, *493*, 673−678.

(9) Papež, Nikola; Dinara, Sobola; Ľubomír, Škvarenina; Pavel, Škarvada; Dušan, Hemzal; Pavel, Tofel; Lubomír, Grmela Degradation analysis of GaAs solar cells at thermal stress. *Appl. Surf. Sci.* **2018**, *461*, 212−220.

(10) Knápek, Alexandr; Jiří, Sýkora; Jana, Chlumská; Dinara, Sobola Programmable set-up for electrochemical preparation of STM tips and ultra-sharp field emission cathodes. *Microelectron. Eng.* **2017**, *173*, 42−47.

(11) Stach, Sebastian; Wiktoria, Sapota; Ştefan, Ţălu; AzinAhmadpourian, Carlos Luna; Ghobadi, Nader; Arman, Ali; Ganji, Mohsen 3-D surface stereometry studies of sputtered TiN thin films obtained at different substrate temperatures. *J. Mater. Sci.: Mater. Electron.* **2017**, *28* (2), 2113−2122.

(12) Arman, Ali; Ţălu, Ştefan; Luna, Carlos; Ahmadpourian, Azin; Naseri, Mosayeb; Molamohammadi, Mehrdad Micromorphology characterization of copper thin films by AFM and fractal analysis. *J. Mater. Sci.: Mater. Electron.* **2015**, *26* (12), 9630−9639.

(13) Ştefan, Ţălu; Morozov, Ilya A.; Yadav, Ram Pratap Multifractal analysis of sputtered indium tin oxide thin film surfaces. *Appl. Surf. Sci.* **2019**, *484*, 892−898.

(14) Ştefan, Ţălu; Bramowicz, Miroslaw; Kulesza, Slawomir; Dalouji, Vali; Solaymani, Shahram; Valedbagi, Shahoo Fractal features of carbon−nickel composite thin films. *Microscopy Res. Technique* **2016**, *79* (12), 1208−1213.

(15) Yadav, R. P.; Kumar, Manvendra; Mittal, A. K.; Pandey, A. C. Fractal and multifractal characteristics of swift heavy ion induced self-affine nanostructured BaF2 thin film surfaces. *Chaos: An Interdisciplinary J. Nonlinear Sci.* **2015**, *25* (8), No. 083115.

(16) Méndez, Alia; Reyes, Yolanda; Trejo, Gabriel; StĘpień, Krzysztof; Ţălu, Ştefan Micromorphological characterization of zinc/silver particle composite coatings. *Microscopy Res. Technique* **2015**, *78* (12), 1082−1089.

(17) Shikhgasan, Ramazanov; Ţălu, Ştefan; Dinara, Sobola; Sebastian, Stach; Guseyn, Ramazanov Epitaxy of silicon carbide on silicon: Micromorphological analysis of growth surface evolution. *Superlattices Microstruct.* **2015**, *86*, 395−402.

(18) SPIP, TM. *"6.7. 4 software (Copyright© 1998−2018 Image Metrology A/S)."* (2019).

(19) Iso, I. S. O. 25178−2:2012—Geometrical Product Specifications (GPS)—Surface Texture: Areal—Part 2: Terms, Definitions and Surface Texture Parameters. *Int. Standards Org.* **2012**, 8−9.

(20) American Society of Mechanical Engineers. *"ASME B46.1−2009. Surface texture (surface roughness, waviness and lay)."* ASME: New York, NY, 2009.

(21) Tsai, Ting-Kan; Chuang, Chia-Chih; Chao, Chuen-Guang; Liu, Wei-Long Growth and field emission of carbon nanofibers on electroless Ni−P alloy catalyst. *Diamond and related materials* **2003**, *12* (9), 1453−1459.

(22) Dalouji, Vali; Ebrahimi, Parisa; Binaei, Nina; Tanhaee, Ehsan; Nezafat, NeginBeryani; Dejam, Laya; Solaymani, Shahram The optical properties of aluminum-doped zinc oxide thin films (AZO): new methods for estimating gap states. *J. Superconductivity Novel Magnetism* **2019**, *32* (5), 1319−1326.

(23) Dalouji, Vali Effect of deposition time on Polaron hopping conduction parameters in carbon films embedded by nickel nanoparticles. *Silicon* **2018**, *10* (6), 2889−2894.

(24) Goudarzi, Samira; Dalouji, Vali The effect of Cu content in MWCNTs synthesized by Ni-Cu@ aC: H catalyst on the optical constants and the optical loss. *Optik* **2020**, *223*, 165585.

(25) Sobola, Dinara, Pavel, Kaspar, Jindrich, Oulehla, Ştefan, Ţălu, Nikola, Papež. "Stereometric analysis of TaO thin films." *Materials Science-Poland* (**2020**).

(26) Garczyk, Żaneta, Sebastian, Stach, Ţălu, Ştefan, Sobola, Dinara, Wróbel, Zygmunt. "Stereometric parameters of butterfly wings." In *Journal of Biomimetics, Biomaterials and Biomedical Engineering*, Vol. *31*, pp 1−10. Trans Tech Publications Ltd, 2017.

(27) Ţălu, Ş.; Contrera-Bulnes, R.; Morozov, I. A.; Rodríguez-Vilchis, L. E.; Montoya-Ayala, G. Surface nanomorphology of human dental enamel irradiated with an Er: YAG laser. *Laser Physics* **2015**, *26* (2), No. 025601.